energies

MDPI

Article

Helical Static Mixer Simulations for Its Integration in the Pour Plate Method: Mixing Agar and a Nutrient Solution

Ana M. Díaz, Inés Terrones-Fernandez, Pedro Javier Gamez-Montero and Robert Castilla *

Department of Fluid Mechanics, Universitat Politecnica de Catalunya, Campus Terrassa, Colom 11, 08222 Terrassa, Spain; ana.maria.diaz.castro@estudiantat.upc.edu (A.M.D.); ines.terrones@upc.edu (I.T.-F.); pedro.javier.gamez@upc.edu (P.J.G.-M.)
* Correspondence: robert.castilla@upc.edu

Abstract: In microbiology laboratories, it is essential to obtain high-quality samples where the culture media are completely homogeneous. The pour plate method includes having to melt the culture media—a mixture of agar and a nutrient solution—before seeding. A static mixer is designed for this purpose, employing CFD (Computational Fluid Dynamics) with the software OpenFOAM to simulate the fluid's behaviour in a helical static mixer with both internal and external configurations. The objective is to validate the CFD model by comparing it with the literature and provide a first approach to the mixer design. After satisfactory validation of the model, the results of the initial designs for Reynolds number 14 reveal the notably different behaviour of the fluids during mixing due to their differing properties, since agar and the nutrient solution present a high viscosity ratio. While the mixing efficiency is similar for the internal and external mixers, improved performance is demonstrated in the internal mixer, even for a shorter version. The external version of the mixer reaches a value for a mixing efficiency of 0.89 whereas the internal version performs more homogeneous mixing for the same number of mixing elements. This evaluation is based on a simplified internal design for computational simulations, whereas the external mixer is easier to manufacture but more complex to implement computationally. Finally, homogeneous mixing is achieved for the internal mixer configuration when adjusting its dimensions to those available on the market.

Keywords: static mixer; helical mixer; Computational Fluid Dynamics (CFD); laminar flow; high viscosity ratio; miscible liquids; mixing index; agar-nutrients; pour plate

Citation: Díaz, A.M.; Terrones-Fernandez, I.; Gamez-Montero, P.J.; Castilla, R. Helical Static Mixer Simulations for Its Integration in the Pour Plate Method: Mixing Agar and a Nutrient Solution. *Energies* **2023**, *16*, 5816. https://doi.org/10.3390/en16155816

Academic Editor: Andrey A. Kurkin

Received: 5 July 2023
Revised: 31 July 2023
Accepted: 3 August 2023
Published: 5 August 2023

1. Introduction

The automation of processes is reaching all fields of science with the aim of facilitating the work of researchers and increasing process efficiency. Microbiology is no exception; it is necessary to automate certain processes carried out in laboratories in order to overcome the obstacles and inconveniences associated with traditional methods.

In the field of food-oriented microbiology, it is common to study the proliferation of microorganisms in Petri dishes filled with culture media. To prepare and deliver the culture media, there are several widely used techniques, including the pour plate method.

The pour plate technique is employed in the field of microbiology for the delivery of a certain quantity of sample onto a sterile Petri dish. Unlike other methods, it permits the deposit of greater amounts of a sample, where colonies form both on the upper layer of the sample as well as in the subsurface. In the traditional method, the preparation or mixture of the gelling agent, melted agar, and nutrient solution can be purchased directly and then manually delivered into the Petri dish, where colonies are left to proliferate in the culture media, kept under adequate conditions [1].

The pour plate method may prove to be a complex process where poor conditions and factors impact the quality of the culture media as well as the survival of the microorganisms. The reference culture media are limited to those available in the market, in addition to

proving to be a notably time-consuming process. An alternative procedure of previously mixing the agar and nutrient solution phases has demonstrated the potential to improve the quality of the culture media sample and expand the possibilities for different culture media compositions and concentrations, e.g., reducing the concentration of agar [1]. This allows for greater flexibility in designing precise culture media formulations adapted to the needs of specific microbiological studies rather than being limited to pre-made agar-nutrient mixes available in the market.

Considering culture media phases as separate entities that can be mixed and then deposited into Petri dishes is an innovative approach that has the potential to revolutionise the current laboratory procedures and traditional pour plate method used in microbiology. Automating the mixing of the two phases would not only increase the quality of the samples but also reduce potential risks and serve as a tool and support for researchers in their studies.

Therefore, the design of a device for the homogenization of culture media is essential, not only for the automation of the process but also because it allows for measurable and demonstrated quality results under simulations instead of directly purchasing the mixture. It is also essential to demonstrate that achieving a culture media equal to the commercial reference is possible when the phases densities and viscosities are notably differing. This device will have the purpose of automatically delivering the final optimum culture media by completing the homogenization of the agar and nutrient phases, in which microorganisms can survive; involving processes and samples that can be reproduced; and avoiding contamination of the media.

In the present work, a novel study based on numerical simulations with the OpenFOAM toolbox is performed. The focus is on the mixing of very viscous fluids or two fluids with a high viscosity ratio. Two kinds of static mixers are considered, one with an internal helical configuration, open design, and the other with an external helical configuration and closed design.

The questions that this study intends to answer are, in the first place, how can the homogenization of the culture media be improved in the pour plate method. It is stated that through automation using a mixing device, reproducible and specific samples can be created and directly delivered in Petri dishes. In addition, it guarantees that there is no cross-contamination and that the mixture of agar and nutrient solution is completely homogeneous.

In the second place, the question arises as to whether two fluids of notably different properties can be mixed to ensure that the final mixture is completely homogeneous? It is demonstrated that, by designing a mixing device and studying its performance using CFD (Computational Fluid Dynamics) to simulate the behaviour and interaction of both fluids, the proposed solution meets the quality requirements for the culture media.

2. Problem Statement

Mixing can then be defined as the process in which two or more substances are combined to form a homogeneous or heterogeneous medium. In addition, if two or more fluids can dissolve completely in each other to form a homogeneous mixture, they are denominated as miscible fluids [2]. The mixing of substances is a fundamental process within a wide range of scientific fields and industries, such as the chemical industry, food, cosmetic, pharmaceutical, materials, composites, and microbiology industries. Despite the importance of such processes in this wide range of fields, there are no standardised technologies or regulations recognised by the scientific community that encompass accepted methodologies and criteria for mixing [2–4].

For the mixing of two liquid species, the devices employed can be classified into passive or static mixers and active mixers. As their name implies, passive or static mixers work by using geometrical features such as baffles, grooves, and channels to create flow perturbations that promote mixing. Active mixers, on the other hand, employ external forces such as electric, magnetic, or acoustic fields to enhance mixing [2–5].

Given the design requirements and integration of the device for the pour plate method, the review of the literature will be solely focused on static mixing devices.

2.1. Static Mixers

Originally, static mixers were created with the aim of reducing the radial thermal gradients present in the mixing processes as well as avoiding the characteristic plug flow effect of laminar flows in which the fluids present very different properties [2].

Commonly, static mixers focus on creating radial flows using baffles and other geometries that enable this motion of the flow. When static mixers are classified by their geometric base design, there are six main types: open design with helices, open design with blades, corrugated plates, multi-layers, closed designs with channels or multi-channels, and a screen or grid [3,4,6].

In order to gain a deeper understanding of the fundamentals upon which the behaviour of two miscible fluids rely during mixing, it is essential to comprehend the effects of the dissipation of energy and pressure drops in mixing devices, as well as the principles that apply in both laminar and turbulent regimes [3].

The pressure drop in a homogeneous, isothermal, and incompressible Newtonian flow is a reliable indicator of the efficiency of static mixers, although it cannot be considered a mixing indicator. This is because it determines the pumping energy required for the process of mixing the substances, which, in turn, affects the overall energy costs [3,7].

To reduce the pressure drop of mixers, it is common practise to employ geometries that allow for lower frictions with walls or the alteration of the shape and dimensions of duct cross-sections, since narrow ducts may increase the pressure drop.

Mixing in laminar flows can be a challenge when compared to turbulent flows due to the fact that the flow remains orderly and undisturbed. Since fluid motion is primarily dominated by linear, viscous forces, the mixing of substances is generally poorer [2,4]. Laminar regimes are common in static mixers when the fluids being mixed are liquid–liquid and present high viscosities, although there are other factors that also affect the Reynolds number and must be assessed.

Consequently, improving the mixing efficiency in laminar flows requires the focus to be placed on the primary flow topology and interphase area. A clear example is the split and recombine method (SAR), in which the flow is divided into several sub-flows that are subsequently recombined, thereby increasing the possibility of mixing by diffusion [2,4]. Other mechanisms for increasing the mixing in laminar flows are the redistribution and twisting of the flow in the radial and tangential directions of the mixer, or the principle of chaotic advection, achieved by variations in the geometries of the mixer, thus obtaining trajectories with continuous direction changes in the fluid [4].

Nevertheless, static mixers may amplify the turbulence that is already present in turbulent flows as well as increase the segregation intensity of radial mixing, which promotes secondary flow creation and the mixing of substances through eddy diffusion (or turbulent diffusion) and convection [2,4].

The dissipation of energy is closely related to the mechanisms of mixing in turbulent flows due to the generation of eddies. There are two mechanisms of energy dissipation in turbulent flow mixing; on the one hand, the dissipation due to viscous boundary layers close to the walls of the mixer; and on the other hand, the dissipation of energy that occurs in the fluid where the core turbulence is homogeneous [4].

2.2. Governing Equations

The equations that govern the fluid are the conservation equations. Adjusting these equations for the mixture of miscible, incompressible Newtonian fluids in a no-slip boundary and considering constant density of the mixture, the expressions in Equations (1)–(3) are obtained [2,7–9]. These expressions refer to the mass conservation, momentum conservation, and species conservation equations, respectively. The momentum conservation equations in the three component directions are usually referred to as the Navier–Stokes

equations. As for the species mass transport equation, it refers to the conservation of a single species; therefore, each species of the multiphase mixture is represented by one of these equations,

$$\nabla \cdot \boldsymbol{v} = 0 \tag{1}$$

$$\frac{\partial \boldsymbol{v}}{\partial t} + \boldsymbol{v} \cdot \nabla \boldsymbol{v} = \mathbf{g} - \frac{1}{\rho}\nabla p + \nu \nabla^2 \boldsymbol{v} \tag{2}$$

$$\frac{\partial c}{\partial t} + (\boldsymbol{v} \cdot \nabla) c = D\nabla^2 c, \tag{3}$$

where $\boldsymbol{v}$ refers to the velocity vector, ρ is the constant effective density, p is the pressure, ν refers to the effective kinematic viscosity, $\mathbf{g}$ is the acceleration of gravity, c refers to the concentration of one of the species, and D is the molecular diffusion coefficient of said species. In turn, the effective density and kinematic viscosity of the mixture can be estimated in terms of the concentration of the species a and b, as expressed in Equations (4) and (5) [8].

$$\rho_{\text{effective}} = c_a \rho_a + c_b \rho_b \tag{4}$$

$$\nu_{\text{effective}} = c_a \nu_a + c_b \nu_b \tag{5}$$

Monitoring and surveillance of spatial and temporal concentrations of the species involved is a widely used method of measurement for macromixing of static mixers due to its efficacy. This technique is also widely employed in computer simulated flow, where a temporal instant and a section of the mixer are chosen in order to record concentration samples. Knowing the concentration map, the mixing index M can be estimated, as expressed in Equation (6). This parameter, also known as mixing ratio or mixing efficiency, represents the degree to which fluids mix with each other until a homogeneous blend is achieved [2,4,5,7,8,10].

$$M = \left(1 - \sqrt{\frac{\sigma^2}{\sigma^2_{\max}}}\right) \tag{6}$$

$$\sigma^2 = \frac{1}{n}\sum_{j=1}^{n}\left(c_i - c_{avg}\right)^2, \tag{7}$$

where $\sigma_{\max}$ is the maximum deviation of the concentration, σ^2 is the sum of variance of the concentration in the spatial reference, n is the number of samples measured, c_i refers to the concentration of each sample, and c_{avg} is the average concentration in the entire spatial reference. Note that a mixing index of 1 implies that both fluids have been completely mixed and there are no traces of unmixed fluids, while a mixing index of 0 implies that none of the fluids have been mixed in the slightest.

2.3. Static Mixers for Highly Viscous Fluids

The mixing of highly viscous fluids or high viscosity ratios between them poses a challenge for the design of an efficient mixer since there is a difference in elongation rate between the fluids, which affects their interphase and, thus, the mixing process [11].

However, there is a dearth of studies and mixer designs specifically focused on such applications, resulting in scant information available, with most references limited to the final product marketed by manufacturers.

Through the study of the market and mixer designs for high viscosities, it has been observed that the sole designs used for these applications are the Kenics model type with helices [12], open designs with blades, and multi-layer and corrugated plate configurations. In their study, Meng et al. (2014) [13] analyse a mixer for a high viscosity ratio in liquid–liquid mixing, using as a reference the Kenics model mixer while also introducing modifications in the number of helices for each mixing element.

From their study, they were able to conclude that a double-helix Kenics mixer is less efficient than a single-helix model due to the presence of unmixed fluid zones. On the

other hand, for triple and quadruple helix configurations, the mixing proved to be more efficient than the original model. Additionally, it was observed that the fluids exhibit resistance to mixing due to the low Reynolds number in laminar flow and high viscosities. Similar effects were also observed in the studies carried out by Regner et al. (2008) [11] for an open design mixer with blades and in the research by Montante et al. (2016) [14] for a section of a SMV-corrugated plate mixer. These studies demonstrate that achieving complete homogenization of high-viscosity fluid mixtures requires intricate mixer designs.

3. Materials and Methods

3.1. Solutions Proposed

Based on the amount of culture media desired to be delivered in each Petri dish and the minimum flow rate to reach this content (0.6 mL/s), it is clear that the flow regime will be laminar. Given the need for a mixer that is simple, easy to produce, and clean, but that also achieves complete homogeneity for the mixture, it is decided to employ the helical static mixer configuration. This type of device enables increasing the efficiency of mixing in both laminar and turbulent regimes since it introduces the effects of centrifugal forces and flow twisting. This decision is based on the advantages that helical mixers present when compared to other types of mixers, especially concerning performance and efficiency versus the simplicity of the design for small and large scale devices.

The two proposed solutions for the helical mixer, according to the inspiration and references taken, are as follows:

- **Internal helical mixer, closed design:** The agar and nutrient phases flow through a square cross-section duct that forms a helical path. This type of internal duct mixer is usually studied in CFD as a modification of the simple T-mixer (STM) that enhances the mixing process [10], keeping relatively simple geometry.
- **External helical mixer, open design:** In this case, the fluid does not flow through a closed square cross-section duct, but it flows through the free spaces existing between an outer cylindrical wall and an interior solid in a spiral form, so that the mixture flows through the exterior of said helical solid. However, although this solution provides a more similar approach to the helical mixers available on the market and is easier to manufacture, it is notably more complex to implement computationally.

3.2. Design Parameters and Mesh Generation

Using a shorter version, with a fewer number of helical elements to analyse the first results, allows for a reduction in the workload and use of resources without sacrificing the quality of the results. However, once the results of each mixing device have been obtained and analysed, it is essential to decide and choose one among them based on their performance in order to run a final simulation with the entire model and study the behaviour of the fluid across the complete length of the duct. In this case, the internal helical mixer has demonstrated a performance closer to the requirements of the design. The main design parameters of each mixer are presented in Table 1, along with their representations in Figure 1.

Table 1. Design parameters and dimensions of the geometries proposed.

Design Parameter [1]	Internal Helical	External Helical	Internal Helical, Entire Device
Hydraulic diameter	2.0	2.7	2.0
Number of mixing elements	4	4	14
Total length	22	22	62
Pitch	4	4	4
External diameter of the helix	7.5	7.5	7.5

[1] Dimensions are expressed in millimetres, except for the number of mixing elements.

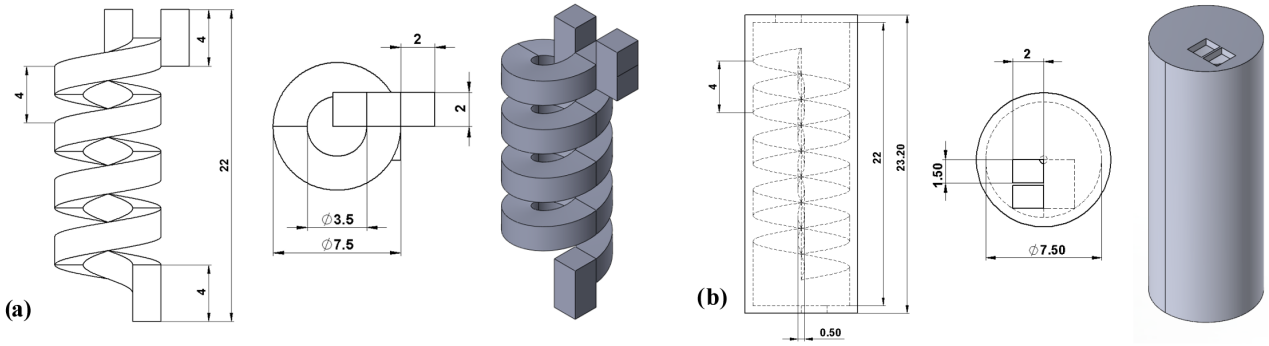

Figure 1. Geometry and dimensions in millimetres of the solutions proposed, front, top, and isometric views, respectively: (**a**) Internal helical mixer. (**b**) External helical mixer.

The meshing of the different mixers is part of the pre-processing stage of the simulations, and two different methodologies have been followed depending on the geometrical complexity of the mixers. For the STM (Simple T-Mixer) employed for the model validation, *blockMesh* has been used, the function integrated directly into OpenFOAM, in order to generate a parametrized mesh where the inputs are simply the dimensions of the mixer and refinement of the mesh. For the helical mixers, the mesh has been generated with Salome due to its features that allow for great adaptability and versatility. Figure 2 shows these meshes for each methodology followed.

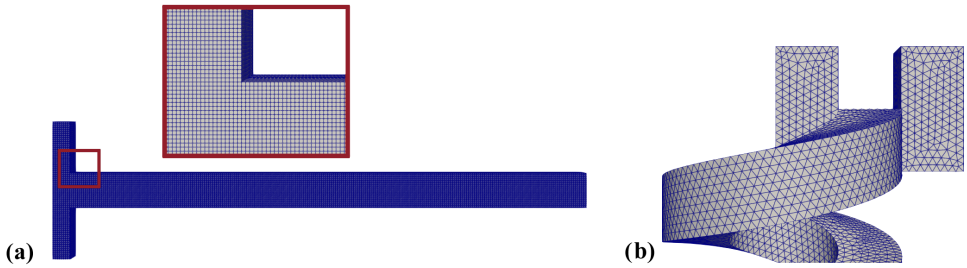

Figure 2. Mesh visualisation for the coarser meshes: (**a**) STM mesh and junction detail. (**b**) Detail of the inlets of the internal helical mixer.

3.3. Model

Given that the case to be studied in this project is the mixing of two incompressible fluids, there is only one solver in OpenFOAM fitting this description; thus, the choice is clear: *twoLiquidMixingFoam* [15].

The two liquids to be mixed are a pre-gelling agar phase and a nutrient phase in a saline or aqueous solution, with the objective of creating a completely homogeneous culture media after mixing them together. The mass fractions of the mixture are 0.5 for the agar phase and 0.5 for the nutrients phase; thus, the amount that is to be introduced into the mixer of each fluid must be the same. The properties of the fluids are presented in Table 2.

Table 2. Property summary for the agar and nutrient solution phases.

Property	Agar Phase	Nutrient Solution Phase
Density (kg/m^3)	1005	1000
Kinematic viscosity (m^2/s)	5.47×10^{-5}	10^{-6}

Given that agar is an uncommon substance with a wide range of properties, the diffusivity coefficient should be estimated experimentally in laboratories. For this reason, it has been decided to take as a reference value the estimations made by Miyamoto et al. (2018) [16] for agar in their study by means of computational simulations, that is, the diffusion coefficient is set to $D = 5 \times 10^{-10}$ m^2/s.

The boundaries defined in the mesh generation are classified into four components: the two inlets, named *inlet1* and *inlet2*, the outlet, defined as *outlet*, and the static mixer duct, defined as *walls*.

The walls have been defined so that the fluid does not slip; therefore, the fluid on the wall must have zero velocity. Additionally, it is specified that the pressure at the outlet is zero in order to more easily estimate the pressure drop. The acceleration of gravity has been defined as 9.81 m/s^2 in the z direction. In regards to the concentration of the species, it is only necessary to define the concentration from 0 to 1 of a single fluid. Consequently, a concentration of 1 implies that the chosen fluid, in this case agar, has not been mixed and is pure, while a concentration of 0 indicates there is a pure concentration of the second fluid, the nutrient solution. Any intermediate concentration value between 0 and 1 implies that both fluids have been mixed. A more detailed description regarding the boundary conditions is presented in Table 3.

Table 3. Boundary conditions summary for the internal helical mixer.

Property Field	*Inlet1*	*Inlet2*	*Outlet*	*Walls*
Velocity [1]	`fixedValue` `uniform (0 0 -0.1)`	`fixedValue` `uniform (0 0 -0.1)`	`pressureInletOutletVelocity` `uniform (0 0 -0.2)`	`noSlip` -
Hydrostatic pressure	`zeroGradient` -	`zeroGradient` -	`fixedValue` `uniform 0`	`zeroGradient` -
Agar concentration	`inletOutlet` `uniform 0`	`inletOutlet` `uniform 1`	`inletOutlet` `uniform 0`	`zeroGradient` -

[1] Note that the velocity magnitude may vary in order to satisfy $Re = 14$ for the internal and external mixers.

The modelling of turbulence is not applicable since the flow regime is laminar. The Reynolds number is estimated to be $Re = 14$ given the average velocity in both internal and external helical mixers, calculated with the mass conservation equation. Given the low Reynolds number in this laminar regime, the definition of a wall function for the resolution of the boundary layer will not be needed; moreover, the meshes created for the mixing of fluids already need high refinement in order to achieve accurate results.

In multiphase simulations, which involve two or more fluids, it is typical to control the iteration time step, by means of the maximum Courant number. Therefore, the iteration time step does not remain constant over the iterations and will depend on many other factors, such as the mesh characteristics or the fluid velocity.

The Courant number is widely used in the CFD field since it can be defined as a measure of the rate of the local flow velocity in an element of the mesh; that is, it defines the quantization of the transport of information given the flow rate in a cell, as defined at *CourantNo* in OpenFOAM User Guide [15]. To control the simulations and the time step, *Co* limits have been established for the explicit MULES algorithm, both for the species fields, $Co_{\alpha,max}$, and for the rest of the fields, Co_{max}.

Lastly, regarding the model, the schemes employed are summarised in Table 4.

Table 4. Schemes summary.

Category	OpenFOAM Keyword	Scheme
First time derivatives ($\partial/\partial t$)	`ddtSchemes`	`Euler`
Gradient (∇)	`gradSchemes`	`Gauss linear`

Divergence ($\nabla\cdot$)	`div(rhoPhi,U)`
	`div(phi,alpha)`
	`div(phi,k)`
	`div(((rho*nuEff)*dev2(T(grad(U)))))`
		`Gauss linear`
		`Gauss vanLeer`
		`Gauss limitedLinear`
		`Gauss linear`

Laplacian (∇^2)	`laplacianSchemes`	`Gauss linear corrected`
Point to point interpolations	`interpolationSchemes`	`Linear`
Component of gradient normal to a cell	`snGradSchemes`	`Corrected`

4. Results and Discussion

4.1. Validation of the Model

In order to validate the results, a comparison with a typical simple mixing model has been researched since this is one of the most widely used simulations due to its simplicity and lower resource needs. For these reasons, a simple T-mixer, also known as STM in this field, has been chosen. Figure 2a illustrates the geometry and mesh of the STM, composed of two inlets and a mixing channel to the outlet, forming a T shape.

The STM has been taken as a reference and is employed by Cortes-Quiroz et al. (2014) [17], Dundi et al. (2019) [18], and Sinha et al. (2022) [10]. These three studies present different results for the same case of mixer geometry and fluid properties for $Re = 266$. This particular case has been chosen because the dimensions, fluid properties, and flow regime are similar to the one that is desired to assess and design in this study. Hence, it is assumed that if the results are validated for the STM, the simulation model generated in OpenFOAM will also be accurate for the simulations of the helical static mixer designed. Note that these authors employ a different software than OpenFOAM, which increases the relevance of result validation in the present study.

In order to simplify simulations, water of the same properties has been chosen as the fluid to be mixed, rather than two different fluids. Water is the most frequent fluid, and its properties are widely known under standard conditions. Therefore, water or Phase A enters through the right inlet at a certain initial velocity, while the second fluid, also water, or Phase B, enters through the left inlet at a certain velocity. Both fluids come into contact with each other perpendicularly; this is where the process of mixing begins. Then, the trajectory and entering of the mixing channel length is changed until reaching the outlet, where the engulfment and mixing of fluids takes place. This phenomenon is shown in Figure 3 for different cross-sections along the mixing channel length.

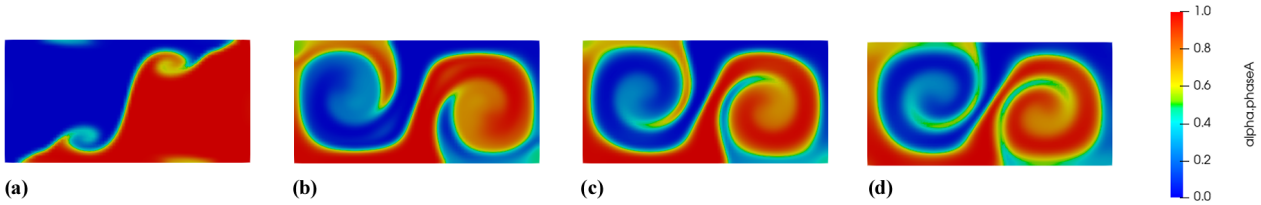

Figure 3. Concentration distribution of the species. Evolution of the engulfment along the mixing channel length for different sections in the STM: (**a**) Section at $x = 0$ µm. (**b**) Section at $x = 500$ µm. (**c**) Section at $x = 1000$ µm. (**d**) Section at $x = 3000$ µm.

Furthermore, the selection of computation sizes was performed through mesh independent test. Figure 4a reveals that, as the number of mesh cells is increased, the resolution and precision of the concentration distribution are improved. The mixing index reduction effect is also presented in the studies carried out by Dundi et al. [18], as the number of cells

is increased. Additionally, the results shown in Figure 4b are again validated with those of Dundi et al. [18]. In their study, Cortes-Quiroz et al. [17] employ the same geometry of the STM under the same fluid conditions, yet with a shorter mixing duct length, obtaining results further from those obtained by Dundi et al. [18] and Sinha et al. [10].

In addition, the results obtained in this study present a tendency notably similar to those of these two latest analyses along the STM duct, with an error of 6–7% for the 5.5 million element mesh. Given the comparatives presented in this section with respect to the literature and the minimum errors in the results, it may be concluded that the model proposed in the present study, including the mesh and OpenFOAM solver, has been successfully validated.

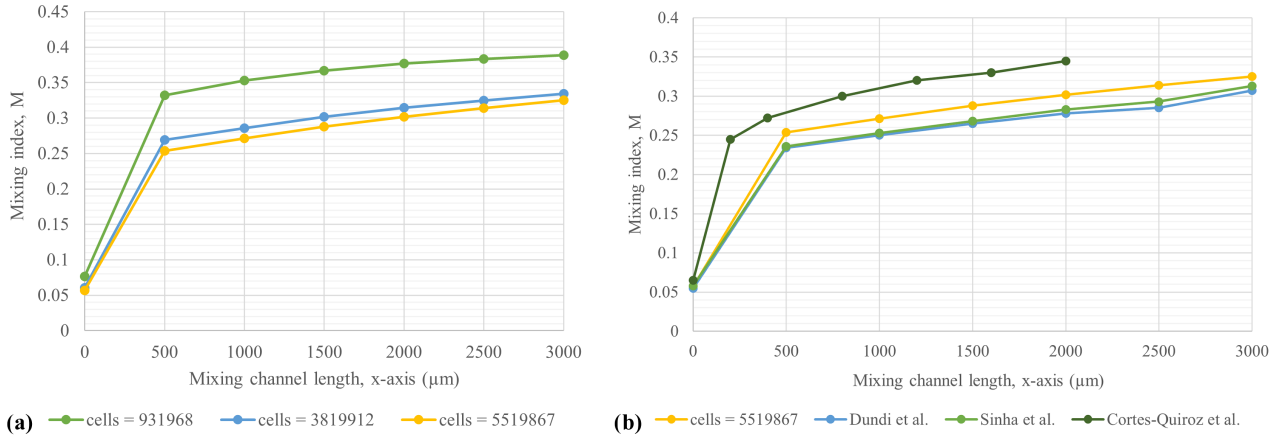

Figure 4. Mixing index for the STM: (**a**) Mixing index for three different meshes. (**b**) Mixing index comparison with literature [10,18].

4.2. Analysis of Solutions: Agar and Nutrient Phase Mixing

4.2.1. Grid Convergence Study

In order to study the grid dependency, five meshes have been generated for the helical mixers, from coarse to fine, where the finer mesh is composed of 795 k cells with a refinement ratio of $r = 1.775$. The reference parameter for the grid convergence study is the mixing index, M, in any cross-section of the helical mixer. It is decided to take section C of the internal helical mixer (see Figure 5a), the first section after completing a revolution of the spiral. The relation between mesh size and mixing index for section C is shown in Figure 6a. Additionally, the mixing index is plotted for the different grid spacings, h_i, of the five meshes studied in this work, along with the Richardson extrapolation at zero grid spacing for $M_{h=0}$ [19], denoted with a red marker in Figure 6b. It is estimated that the finer mesh error in relation to the extrapolation is approximately 6%.

To distinguish if the results obtained for the mixing index are asymptotic and ensure grid convergence, the GCI (Grid Convergence Index) relation between the coarse and fine meshes should tend to 1 [19]. The result presented in Equation (8) demonstrates that the behaviour of the mesh still presents a certain margin for improvement but that the results can already be taken into consideration. Nonetheless, increasing the number of cells in the meshes is a process that falls outside the scope of this study with its available resources.

$$\frac{GCI_{2,3}}{r^p \times GCI_{1,2}} = 0.89, \tag{8}$$

where p is the order of convergence, $GCI_{1,2}$ refers to the grid convergence index of the fine and medium meshes, and $GCI_{2,3}$ refers to the medium and coarse meshes index.

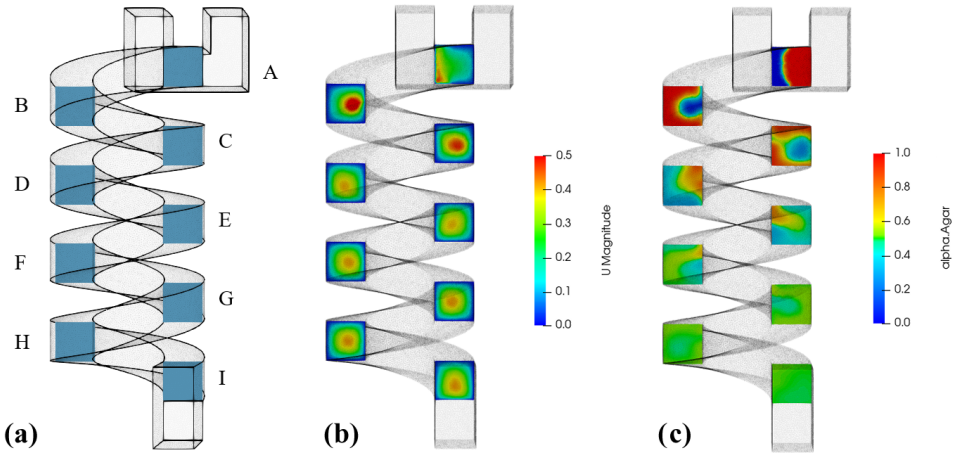

Figure 5. Results for the internal helical mixer: (**a**) Cross-section nomenclature. (**b**) Velocity field (m/s). (**c**) Concentration distribution.

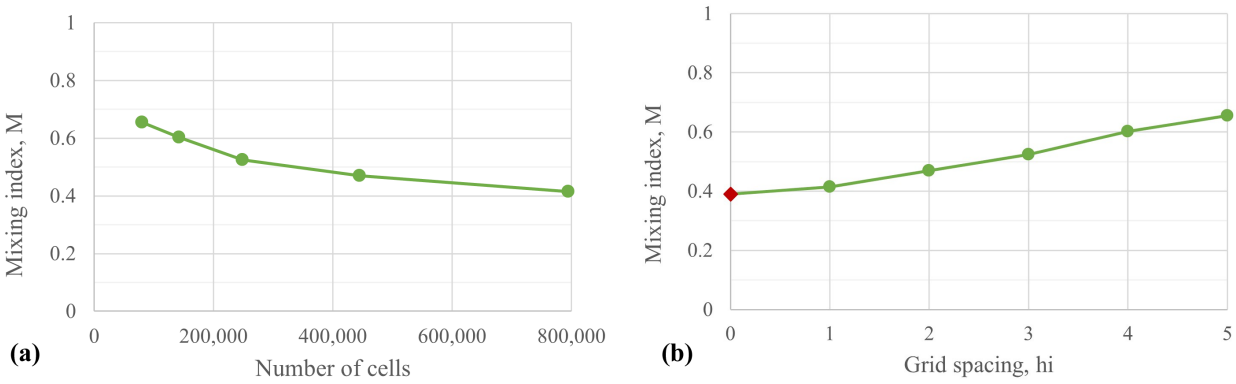

Figure 6. Mixing index at section C of the internal helical mixer: (**a**) For different mesh sizes. (**b**) For different grid spacings, h_i, where i refers to each mesh.

The final residuals, in the order of 10^{-7} to 10^{-8}, especially with regards to the agar concentration with 10^{-12}, and the property field resolution in time, can be considered highly satisfactory and meet the minimum simulation requirements.

4.2.2. Internal Helical Mixer

Given that the internal mixer analysis must be orientated to the performance of both the fluids separately and the behaviour of the mixture, it is necessary to previously define a nomenclature which helps to study the properties of the fluids by sections, as observed in Figure 5a.

Any intermediate value implies a mixing of the fluids, where the target or ideal homogenisation refers to a concentration of the agar phase equal to 0.5, given that the same amount of agar and nutrients phases is introduced into the mixer.

It is essential to understand the fact that the two fluids presenting notably different viscosities will undoubtedly affect the velocity field, given that the more viscous fluid, the agar in this case, presents higher resistance to motion and shear forces, whereas the nutrient phase, being less viscous, will attain higher velocities. Nonetheless, since the velocity and Reynolds number are low, the effects of centripetal forces are not as noticeable as they could be at higher static mixer flow rates. These results are presented in Figure 5b.

Additionally, it can also be observed that the maximum velocity values, which are predominantly present in the initial sections and correspond to the nutrient phase zone, are smoothed as the species flow along the mixer.

In Figure 5, two key factors influencing the behaviour of the fluids in this helical mixer can clearly be observed:

1. The engulfment of the nutrient solution (blue fluid) by the agar (red fluid), due to the difference in viscosity, starts from the very first cross-sections, where the plug flow is clearly visible in sections B and C in Figure 5c.
2. The maximum values on the velocity field correspond to the nutrient phase, while the minimum values for the velocity, apart from the zero velocity at the wall, refer to the agar phase.

It can be observed in sections A, B, and C, as the fluids are not yet mixed with a notable difference in viscosities, that the nutrient phase tends to concentrate and be located in the centre of the duct. On the other hand, agar, with a viscosity 55 times greater than the fluids, resists motion due to friction from the walls and completely envelops the nutrient phase. This phenomenon is known as the plug flow, and it usually takes place when mixing fluids with very different properties in curved ducts. Additionally, with every revolution of the spiral flow, twisting takes place, increasing the mixing of the fluids, where the target homogenisation refers to a concentration of the agar phase equal to 0.5, given that the same amount of agar and nutrient phases is introduced into the mixer.

The effects of centrifugal force and nutrient engulfment by the agar cause the interface area to become larger and significantly altered with each revolution of the helix. Consequently, the mixing of the agar and nutrients is led mainly by diffusion but is without doubt increased by the geometry of the spiral mixer and flow twisting.

Similar effects on the flow through helical mixers have also been experienced during their simulations in the studies carried out by Sinha et al. (2022) [10] and Liu et al. (2013) [20]. However, in their studies, they used two equal fluids for the mixing analysis; therefore, no viscosity difference is present and the plug flow effect does not occur.

Furthermore, although it is not clearly visible in the concentration distribution for the different sections, the presence of bubbles or irregularities in the fluid distribution can be demonstrated due to the high difference between viscosities. That is, at certain parts or curves of the helical mixer, there is a greater amount of one fluid than the other, even though the inlet flow rate is the same for both fluids. This can be observed, for example, in section B, where the agar flow rate is notably higher than that of the nutrients, whereas in section E the opposite occurs, where the amount of nutrients is greater than that of the agar.

Despite this, the presence of these bubbles and irregularities does not affect the outflow rate or the final mixing of the fluids, as can be observed from the cross-section I at the outlet, where both fluids are practically completely mixed and the final culture media is nearly homogeneous. Based on these results, data processing is used to approximately estimate the pressure drop, at $\Delta P = 4$ kPa.

Calculations of the mixing index are carried out by taking samples across the entire area of each of the sections, measuring between 1100 and 1200 samples for each cross-section, which are coincident with the points of the mesh. Using Equation (6), the mixing index, M, is estimated along the channel length of the mixer and represented in Figure 7.

This graph illustrates how the mixing index increases rapidly as it passes through the cross-sections until it asymptotically tends towards one; however, it does not reach a complete mixing ratio, as it was found that in the outlet, the mixing index is $M = 0.98$.

4.2.3. External Helical Mixer

The agar phase and the nutrient phase enter their respective inlets vertically, in contrast to the internal mixer, where both fluids come into contact at the horizontal junction. During the early instants, it can be observed in Figure 8c that a fraction of both fluids do not pass through the first revolution of the spiral, as they are directed straight to the second mixing element, from section A to section B. The other fraction of the fluids do flow through the spiral normally. In this first part of the mixer, the viscosity difference is becoming evident, especially how the agar tends to adhere to the walls due to friction effects.

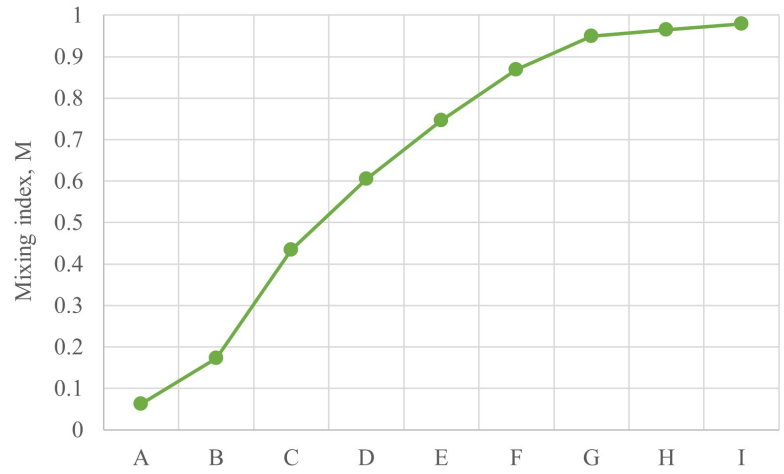

Figure 7. Mixing index for every cross-section of the internal helical mixer (see Figure 5a for further detail on section nomenclature).

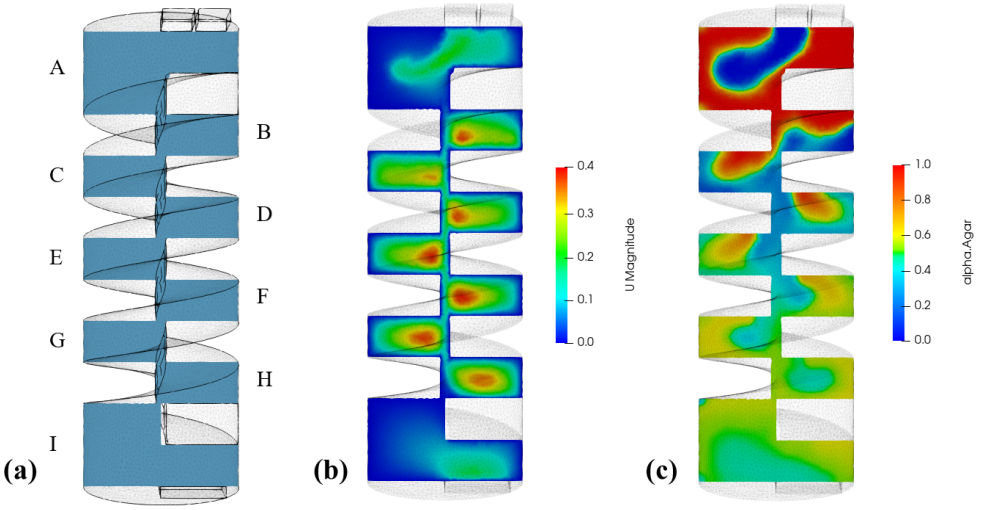

Figure 8. Results for the external helical mixer: (**a**) Cross-section nomenclature. (**b**) Velocity field (m/s). (**c**) Concentration distribution.

Additionally, due to the design of the geometry of the external helical mixer, there is a certain central cylindrical cavity through which a part of the fluid flows. During the design stages, several iterations have been made to the 3D model of this mixer in order to reduce the central diameter as much as possible, thus avoiding any issues regarding geometry tolerances and mesh quality. However, some of the liquids flow through this central section, preventing them from passing through the mixing elements and rejoining the spiral on certain occasions. This filtration presents an inconvenience for the external mixer since it does not enable the fluids to come into adequate contact and thus not mixing correctly.

The relation between the velocity and the concentration of the fluids is clear: the least viscous fluid, the nutrients, reach higher velocities than the most viscous fluid, the agar; thus, the agar tends to envelope the nutrients, which are flowing in the centre of the section. Therefore, the previously mentioned plug flow appears. The effect of the centripetal forces on the fluids, both before and after their mixing, is more evident in the velocity field when compared to the internal helical mixer, since the peak of the velocity profile shifts slightly towards the centre due to the reduction of the inner radius of the helix.

In addition, areas of fluid stagnation can be observed at cross-sections A and I in Figure 8b, where velocities are practically zero further from the inlets and the outlet. This effect is undoubtedly due to the geometry of the external helical mixer and the difference in viscosity between the fluids. The fact that the fluids remain stagnant in these areas can

be a cause for concern for the performance of the mixer; hence, it is necessary to study in more detail the behaviour of the fluids in these sections.

This stagnation of fluids can affect the final concentration of the mixture, as the agar has a tendency to adhere to the walls due to its viscosity. This, in turn, affects the final outcome of the culture media. Furthermore, areas are formed where residues of the fluid remain, which can damage and contaminate subsequent mixtures and procedures for the next Petri dish.

The pressure drop can be estimated with the available data approximately as $\Delta P = 1.4$ kPa. The difference in pressure drop with respect to the internal mixer is drastic, taking into account that the pressure drop in mixers presenting the same mixing index is a fundamental parameter, since a lower pressure drop corresponds to a higher mixing efficiency. This represents an advantage of the external design over the internal mixer. Nevertheless, since in this case the mixers do not achieve a similar mixing index, it is not possible to use the pressure drop as a comparison parameter for mixing efficiency.

Images in Figure 8 show that the engulfment of agar and nutrients and the plug flow reappear due to the difference in the viscosity of the fluids; however, the effects are not as clear as in the internal mixer since, in this case, the liquid that flows through the central section without mixing, reinteracting with the fluid that is passing through the spiral, interferes. Nonetheless, the flow twisting is remarkable, which helps to vary and increase the interphase area of the fluids; therefore, the fluids can be more easily mixed by diffusion.

Figure 9 shows the same asymptotic tendency that had been observed in previous results for other mixers; however, at the last cross section of the mixer, only a mixing index of 0.89 was achieved, far from the target mixing index, $M = 1$. If the tendency of the mixing index is analysed in each section, it can be inferred that additional mixing elements would be necessary just to reach the same value as obtained at the outlet of the internal helical mixer.

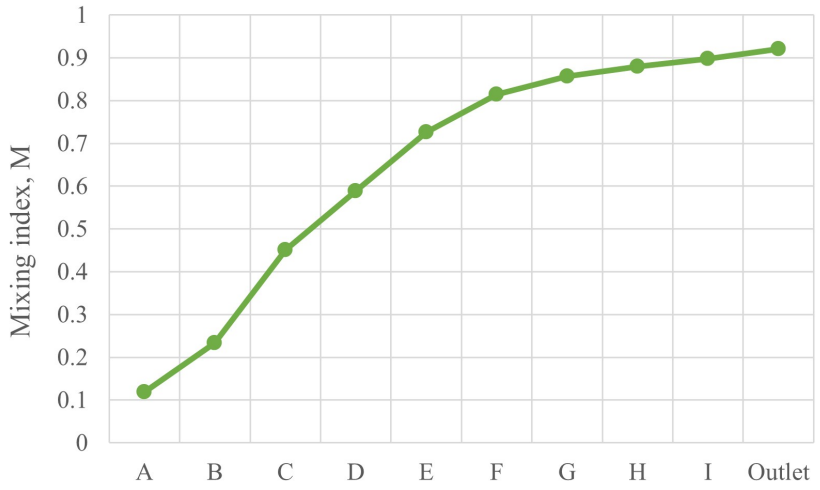

Figure 9. Mixing index for every cross-section of the external helical mixer (see Figure 8a for further detail on section nomenclature).

4.2.4. Entire Model of the Internal Helical Mixer

In light of the results obtained for the internal and external helical mixers, it is decided to simulate the behaviour of the entire internal mixer device by increasing its length and number of mixing elements. Moreover, the entire model of the internal mixer is a design closer to those available on the market in terms of dimensions. This decision is based on the fact that, unlike the external mixer, the internal mixer does not present considerable fluid stagnation that could contaminate the final culture media, using simpler geometries that also manage to reach a much higher mixing index. However, it must be considered that actual mixers are more similar to the external mixer geometry, since it is notably easier to produce and manufacture for a slightly poorer performance.

The agar phase's high viscosity has a noticeable effect on the pressure drop due to friction with the walls of the duct. In contrast, the nutrient phase has no significant effect on the pressure drop due to friction, and can therefore be regarded as negligible. Hence, the resulting total pressure drop is $\Delta P = 11.8$ kPa. As expected, the pressure drop is almost three times that of the reduced version mixer due to the increased length of the duct.

The principles of the behaviour of the fluids during the mixing process are the same as those observed in the simulations for the reduced internal mixer. In Figure 10, it can be observed once again that, from the entrance of the mixer, the most viscous fluid, which is the agar phase, envelops the nutrients phase towards the centre of the section, which is known as the plug flow. The difference in viscosity between the fluids is the cause of both the plug flow and the velocity field. The nutrients initially acquire a higher velocity due to being less viscous and offering less resistance due to friction, in contrast to the agar.

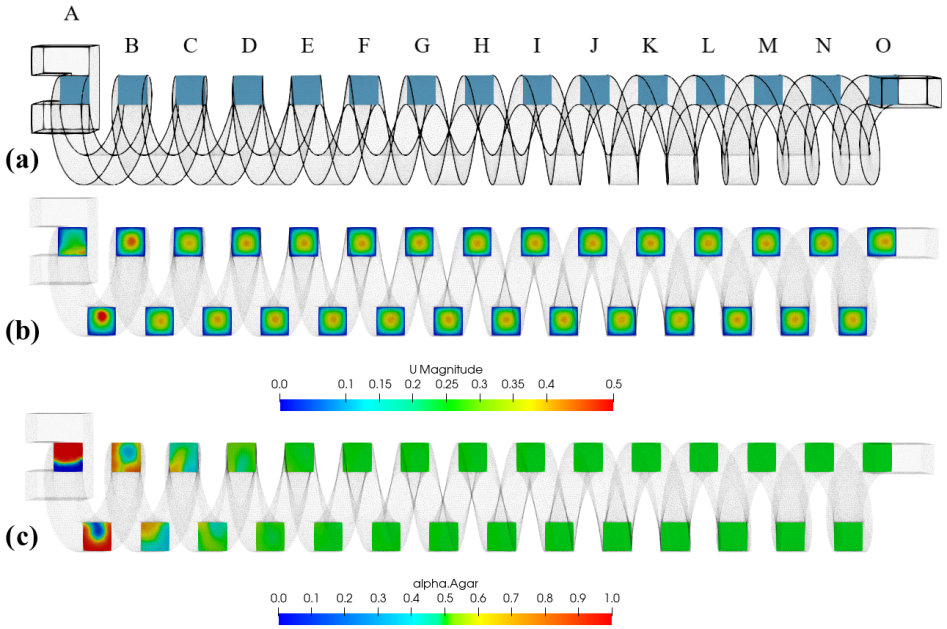

Figure 10. Results for the entire model of the internal helical mixer: (**a**) Cross-section nomenclature. (**b**) Velocity field (m/s). (**c**) Concentration distribution.

Figure 11 illustrates that the mixing index for the sections between A and E coincides with that obtained for the reduced version of the internal helical mixer. With a higher number of cross-sections reaching the complete mixing of the fluids to attain the final culture media, it is possible to observe the asymptotic behaviour of the mixing index towards 1.

In view of these results, it can be observed that the agar and nutrients mix quickly in the first mixing elements, but it is not until Section I that it can be considered that the fluids have been completely mixed, with a mixing index of $M = 0.998 \simeq 1$, allowing for an error in calculations and estimations of 0.2%.

These results imply that to complete the homogenization process of the agar and nutrient phases, only eight mixing elements are required, given the rest of the design parameters and dimensions. The complete mixing is obtained before reaching 60% of the total length of the mixer; thus, it could even be considered to reduce the total number of mixing elements by 2 or 3, thereby reducing the pressure drop and size of the device.

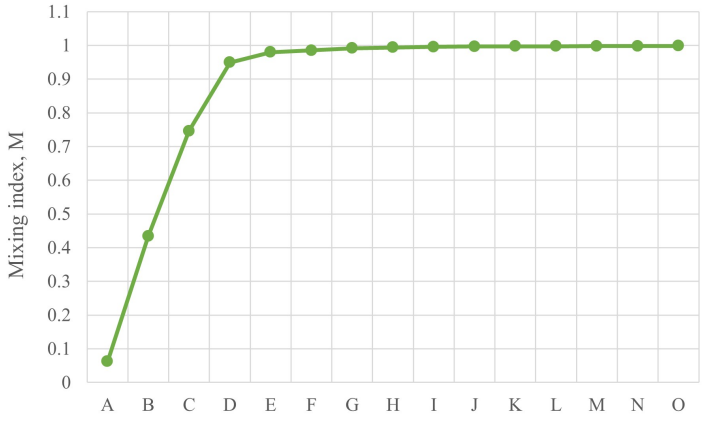

Figure 11. Mixing index for every cross-section of the entire model of the internal helical mixer (see Figure 10a for further detail on section nomenclature).

5. Conclusions

During the research stage on the project's subject matter, it became evident that there is a great deal of information concerning static mixers, yet there are few studies from a Computational Fluid Dynamics perspective on fluid mixing. Therefore, there is still room for research on the mixing of fluids and how to simulate fluid interactions computationally.

Moreover, the two solutions proposed for the design of the static mixer have shown the potential to meet the minimum design requirements established. The first solution proposed is a closed helical design, that is, an internal helical mixer as a simplified version of a regular static mixer oriented to CFD simulations. The second solution considered is an open helical design or external helical mixer, which is closer to real life mixers such as those from the Kenics series by Chemineer.

Nevertheless, the results have brought to light the different advantages and disadvantages of each mixer model. On the one hand, the internal helical mixer has been demonstrated to offer better results in terms of quality and performance in the mixing process, reaching a mixing index of $M = 0.98$ for four mixing elements; however, its geometry implies a more complex manufacturing process. Thus, these types of mixers are more suitable as an equivalence in CFD simulations.

On the other hand, the external mixer is easier to manufacture and could potentially provide a similar performance to the internal mixer when fixing the issues of stagnant fluid residuals and flow of unmixed fluid through the central section. However, the complexity of the simulation and design in regard to CFD is high when compared to the results achieved, attaining a mixing index of $M = 0.89$, in contrast with the internal design, which performs a more homogeneous mixing for the same number of mixing elements. This mixing index differs from the objective by 11%, while the internal helical mixers present a 2% deviation from the target mixing.

For these reasons, it has been decided to ultimately study the complete geometry of the internal mixer, increasing the number of mixing elements; this has proven to meet the design requirements satisfactorily. By increasing the number of mixing elements in the mixer, it is possible to reach a completely uniform culture media within just 60% of the total length of the mixer, proving a negligible deviation of 0.2% from the target mixing. Although the outcomes have been fully satisfactory, further iterations of both designs will be necessary in order to obtain an optimum device that is suitable for its use in microbiology and its integration in laboratories.

While this computational model is applicable to a wide variety of cases for solving the behaviour of the fluids during mixing, it also presents certain limitations. In the first place, the present model is limited to only two fluids, which must also be incompressible and are applicable exclusively in laminar flow regimes. Furthermore, the case of two separate inlets for each fluid and a single outlet has only been considered.

Experimental validation of numerical results can also be very valuable. Little information has been found on experimental methods in this kind of device, and the methods are basically divided into two kinds. The fist method involves chemical reactions [21]. The second is based on Image Processing with quasi-two dimensional devices [22–24]. Both methodologies will be explored in future work to obtain experimental results on the mixing efficiency of these devices.

The design of the mixers, both internal and external, can be improved based on the results obtained in the present study. In addition, it is proposed to study the effect of the cross-section shape, pitch, and diameter of the helix, as well as other design parameters of the mixer. A future proposed project on this matter is the Design of Experiments (DoE) using CFD to study the effects of mixer geometry on the mixing index, with the aim of obtaining an optimal ratio of mixing efficiency to geometric simplicity. The effect of different flow rates and, hence, velocities will also be explored.

After several iterations in the design of simpler static mixers, it would be interesting to move on to the study of more complex geometries. From the market research, it has been observed that mixers from the Kenics series and the multi-layer SMX series can offer better performance for mixing fluids with high viscosity ratios. Therefore, it is proposed to investigate a reduced and simplified version of both models.

Author Contributions: Conceptualisation, A.M.D., I.T.-F., P.J.G.-M. and R.C.; methodology, A.M.D., I.T.-F., P.J.G.-M. and R.C.; software, A.M.D.; validation, A.M.D., P.J.G.-M. and R.C.; writing—original draft preparation, A.M.D.; writing—review and editing, A.M.D., I.T.-F., P.J.G.-M. and R.C.; supervision, P.J.G.-M. and R.C.; project administration, P.J.G.-M. and R.C. All authors have read and agreed to the published version of the manuscript.

Funding: This research was funded by Doctorats Industrials from Generalitat de Catalunya grant number 2021 DI 42. The APC was funded by Doctorats Industrials from Generalitat de Catalunya.

Data Availability Statement: Not applicable.

Acknowledgments: The authors would like to acknowledge the Generalitat de Catalunya for providing the necessary support to the research groups IAFARG (SGR 286, https://iafarg.upc.edu, accessed on 28 June 2023), CATMech (Tecnio, https://catmech.upc.edu/home, accessed on 28 June 2023).

Conflicts of Interest: The authors declare no conflict of interest.

References

1. Terrones-Fernandez, I.; Casino, P.; López, A.; Peiró, S.; Ríos, S.; Nardi-Ricart, A.; García-Montoya, E.; Asensio, D.; Marqués, A.M.; Castilla, R.; et al. Improvement of the Pour Plate Method by Separate Sterilization of Agar and Other Medium Components and Reduction of the Agar Concentration. *Microbiol. Spectr.* **2023**, *11*, e03161-22. [CrossRef] [PubMed]
2. Paul, E.; Atiemo-Obeng, V.; Kresta, S. *Handbook of Industrial Mixing: Science and Practice*; John Wiley & Sons, Ltd.: Hoboken, NJ, USA, 2004. [CrossRef]
3. Valdés, J.; Kahouadji, L.; Matar, O. Current advances in liquid–liquid mixing in static mixers: A review. *Chem. Eng. Res. Des.* **2022**, *177*, 694–731. [CrossRef]
4. Ghanem, A.; Lemenand, T.; Valle, D.D.; Peerhossaini, H. Static mixers: Mechanisms, applications, and characterization methods—A review. *Chem. Eng. Res. Des.* **2014**, *92*, 205–228. [CrossRef]
5. Cetkin, E.; Miguel, A. Constructal branched micromixers with enhanced mixing efficiency: Slender design, sphere mixing chamber and obstacles. *Int. J. Heat Mass Transf.* **2019**, *131*, 633–644. [CrossRef]
6. Thakur, R.; Vial, C.; Nigam, K.; Nauman, E.; Djelveh, G. Static mixers in the process industries—A review. *Chem. Eng. Res. Des.* **2003**, *81*, 787–826. [CrossRef]
7. Su, Y.; Lautenschleger, A.; Chen, G.; Kenig, E. A numerical study on liquid mixing in multichannel micromixers. *Ind. Eng. Chem. Res.* **2014**, *53*, 390–401. [CrossRef]
8. Alam, M.M.; Watanuki, K.; Takao, M. Numerical Analysis of Two-Liquid Flow in a Micro-Spiral Channel. In *Lecture Notes in Mechanical Engineering*; Springer: Berlin/Heidelberg, Germany, 2020; pp. 297–304. [CrossRef]
9. Prakash, R.; Zunaid, M.; Samsher. Simulation analysis of mixing quality in T-junction micromixer with bend mixing channel. *Mater. Today Proc.* **2021**, *47*, 3833–3838. [CrossRef]
10. Sinha, A.; Zunaid, M.; Tokas, S.; Ansari, M. Numerical study of microscale passive mixing in a 3-Dimensional spiral mixer design. *Mater. Today Proc.* **2022**, *56*, 851–856. [CrossRef]

11. Regner, M.; Östergren, K.; Trägårdh, C. Influence of viscosity ratio on the mixing process in a static mixer: Numerical study. *Ind. Eng. Chem. Res.* **2008**, *47*, 3030–3036. [CrossRef]
12. Nov, K. Kenics Static Mixers and Heat Exchangers. Available online: https://www.nov.com/products-and-services/brands/kenics (accessed on 25 May 2023).
13. Meng, H.; Wang, F.; Yu, Y.; Song, M.; Wu, J. A numerical study of mixing performance of high-viscosity fluid in novel static mixers with multitwisted leaves. *Ind. Eng. Chem. Res.* **2014**, *53*, 4084–4095. [CrossRef]
14. Montante, G.; Coroneo, M.; Paglianti, A. Blending of miscible liquids with different densities and viscosities in static mixers. *Chem. Eng. Sci.* **2016**, *141*, 250–260. [CrossRef]
15. OpenFOAM User Guide. Documentation, User Guide, Version 10. Available online: https://www.openfoam.com/documentation/user-guide (accessed on 22 May 2023).
16. Miyamoto, S.; Atsuyama, K.; Ekino, K.; Shin, T. Estimating the Diffusion Coefficients of Sugars Using Diffusion Experiments in Agar-Gel and Computer Simulations. *Chem. Pharm. Bull.* **2018**, *66*, 632–636. [CrossRef] [PubMed]
17. Cortes-Quiroz, C.; Azarbadegan, A.; Zangeneh, M. Evaluation of flow characteristics that give higher mixing performance in the 3-D T-mixer versus the typical T-mixer. *Sens. Actuators B Chem.* **2014**, *202*, 1209–1219. [CrossRef]
18. Dundi, T.; Raju, V.; Chandramohan, V. Numerical evaluation of swirl effect on liquid mixing in a passive T-micromixer. *Aust. J. Mech. Eng.* **2019**, *19*, 363–377. [CrossRef]
19. NASA Glenn Research Center. Examining Spatial (Grid) Convergence. Available online: https://www.grc.nasa.gov/www/wind/valid/tutorial/spatconv.html (accessed on 2 May 2023).
20. Liu, K.; Yang, Q.; He, S.; Chen, F.; Zhao, Y.; Fan, X.; Li, L.; Shan, C.; Bian, H. A High-Efficiency Three-Dimensional Helical Micromixer in Fused Silica. *Microsyst. Technol.* **2013**, *19*, 1033–1040. [CrossRef]
21. Soleymani, A.; Kolehmainen, E.; Turunen, I. Numerical and experimental investigations of liquid mixing in T-type micromixers. *Chem. Eng. J.* **2008**, *135*, S219–S228. [CrossRef]
22. López, R.R.; Sánchez, L.M.; Alazzam, A.; Burnier, J.V.; Stiharu, I.; Nerguizian, V. Numerical and experimental validation of mixing efficiency in periodic disturbance mixers. *Micromachines* **2021**, *12*, 1102. [CrossRef] [PubMed]
23. Wang, H.; Yang, K.; Wang, H.; Wu, J.; Xiao, Q. Statistical Image Analysis on Liquid-Liquid Mixing Uniformity of Micro-Scale Pipeline with Chaotic Structure. *Energies* **2023**, *16*, 2045. [CrossRef]
24. Zhou, D.; Qin, L.; Yue, J.; Yang, A.; Jiang, Z.; Zheng, S. Numerical and experimental investigations of spiral and serpentine micromixers over a wide Reynolds number range. *Int. J. Heat Mass Transf.* **2023**, *212*, 124273. [CrossRef]